

Matrix algorithms for solving (in)homogeneous bound state equations

M. Blank, A. Krassnigg

*Institut für Physik, Universität Graz,
Universitätsplatz 5, 8010 Graz, Austria*

Abstract

In the functional approach to quantum chromodynamics, the properties of hadronic bound states are accessible via covariant integral equations, e.g. the Bethe-Salpeter equations for mesons. In particular, one has to deal with linear, homogeneous integral equations which, in sophisticated model setups, use numerical representations of the solutions of other integral equations as part of their input. Analogously, inhomogeneous equations can be constructed to obtain off-shell information in addition to bound-state masses and other properties obtained from the covariant analogue to a wave function of the bound state. These can be solved very efficiently using well-known matrix algorithms for eigenvalues (in the homogeneous case) and the solution of linear systems (in the inhomogeneous case). We demonstrate this by solving the homogeneous and inhomogeneous Bethe-Salpeter equations and find, e.g. that for the calculation of the mass spectrum it is more efficient to use the inhomogeneous equation. This is valuable insight, in particular for the study of baryons in a three-quark setup and more involved systems.

Keywords: Bethe-Salpeter equation, Faddeev equation, integral equation, solution methods

1. Introduction

The underlying quantum field theory of the strong interaction in the standard model of elementary particle physics is quantum chromodynamics (QCD), a non-abelian gauge theory which deals with elementary degrees of freedom called quarks and gluons [1]. A remarkable feature of QCD is asymptotic freedom, which means that the running coupling of the theory is small in the high-energy regime [2–4]. There, perturbation theory can be applied, and perturbative QCD has been well established in the high-energy domain, (e.g. [5] and references therein). At low energies, however, perturbation theory is no longer applicable, since the value of the running coupling increases to the order of 1. Since bound states are intrinsically nonperturbative, corresponding methods have been developed and used to investigate hadrons, the bound states of quarks and gluons. We eclectically list a few references regarding constituent quark models [6–10], effective field theories [11–13], lattice-regularized QCD [14–19], QCD sum rules [20–25], and the renormalization-group approach to QCD [26, 27] (always see also references therein).

Another remarkable property closely related to bound states is the so-called confinement of quarks and gluons. It entails that only objects like hadrons, where the color charges carried by the elementary degrees of freedom are combined to a color-neutral state, can be observed directly.

While in constituent-quark models confinement is usually implemented via potential terms of an infinitely rising nature (of, e.g., harmonic-oscillator or linear type), in QCD the particularities are more delicate (for a recent review of the problems surrounding quark confinement, see e.g. [28]). In a quantum field theoretical setup, as we use it here, confinement is tied to the properties of the fundamental Green functions of the theory.

In the present work, we employ the Dyson-Schwinger-equation (DSE) approach to QCD. The DSEs are the covariant and nonperturbative continuum equations of motion in quantum field theory. They constitute an infinite set of coupled and in general nonlinear integral equations for the Green functions of the quantum field theory under consideration. There are several extensive reviews on the subject that focus on different aspects of DSEs, like fundamental Green functions [29–31], bound-state calculations [32, 33] and applications of the formalism, e.g. to QCD at finite temperature and density [34]. Bound states are studied in this approach with the help of covariant equations embedded in the system of DSEs. In particular, the Bethe-Salpeter equation (BSE) [35, 36] is used for two-body problems such as mesons [37–39] and covariant Faddeev-type equations [40] are used for three-body problems such as baryons [41].

Ideally, one could obtain a self-consistent simultaneous solution of all DSEs, which would be equivalent to a solution of the underlying quantum field theory. While in investigations of certain aspects of the theory such an approach is successful (see, e.g. [42, 43] and references therein), numerical studies of hadrons necessitate a trun-

Email address:

`martina.blank@uni-graz.at` `andreas.krassnigg@uni-graz.at`
(M. Blank, A. Krassnigg)

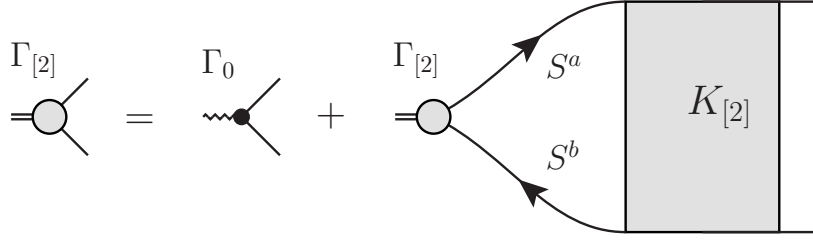


Figure 1: The inhomogeneous vertex BSE, Eq. (1)

cation of this infinite tower of equations.

Once the covariant bound-state equation has been solved to obtain the mass spectrum of the system under consideration, the corresponding covariant amplitudes can be used to compute further observables. In rainbow-ladder truncation, prominent examples include leptonic decay constants [44–46], hadronic decays [47, 48], and electromagnetic properties of both mesons [49–53] and baryons [54–59]. Improvements to this truncation have been considered in the past and studies in this direction are under way [60–65]. What we discuss in the present work is most easily exemplified in a simple truncation, but becomes more important — and thus relevant — with any kind of increasing numerical effort necessitated by either a more involved truncation or the study of a system of more than two constituents.

The paper is organized as follows: in sec. 2 we collect the necessary formulae regarding covariant bound-state equations as they are obtained in the DSE approach to QCD. Section 3 details the discretization of the integrals and the general numerical setup. Section 4 contains numerical solution strategies for both the homogeneous and inhomogeneous bound state equations. In sec. 5 we apply the methods described to solve the homogeneous and inhomogeneous BSE for pseudoscalar mesons in rainbow-ladder truncation and analyze the efficiency of the algorithms. Conclusions and an outlook indicating both immediate and further possible applications of the strategies described herein are offered in sec. 6.

All calculations are performed in Euclidean space.

2. Structure of covariant bound-state equations

In the DSE approach to QCD, mesons are described by general vertices connecting (anti-)quarks to objects carrying the appropriate quantum numbers as demanded by the respective superselection rules. These vertices are the so-called (inhomogeneous) Bethe-Salpeter amplitudes (BSAs), denoted by $\Gamma_{[2]}(k, P)$, which describes a two-particle system, denoted by the subscript $[2]$, with total momentum P and relative momentum k of the constituents. The inhomogeneous BSA satisfies the inhomogeneous

vertex BSE,

$$\Gamma_{[2]}(k, P) = \Gamma_0(k, P) + \int_q K_{[2]}(k, q, P) S^a(q_+) \Gamma_{[2]}(q, P) S^b(q_-), \quad (1)$$

where $\Gamma_0(k, P)$ is a driving term with the quantum numbers of the system, the Euclidean-space four-dimensional momentum integration is given by $\int_q = \int \frac{d^4 q}{(2\pi)^4}$, $S^{a,b}(q_{\pm})$ denote the renormalized dressed (anti-)quark propagators, $K_{[2]}(k, q, P)$ represents the quark-antiquark interaction kernel, and $q_{\pm} = q \pm \eta_{\pm} P$ are the (anti-)quark momenta with momentum partitioning η_{\pm} such that $\eta_+ + \eta_- = 1$, respectively. The choice of the momentum partitioning is arbitrary and usually a matter of convenience, e.g., for equal-mass constituents a convenient choice is $\eta_+ = \eta_- = 1/2$. A graphical representation of Eq. (1) is given in Fig. 1, where the arrows denote dressed-quark propagators (analogously in Figs. 2 and 3).

The solution of (1), $\Gamma_{[2]}(P, k)$, contains both off-shell and on-shell information about the states in a channel with the quantum numbers under consideration, which are fixed via the construction of $\Gamma^0(k, P)$ and $\Gamma_{[2]}(P, k)$. In particular, $\Gamma_{[2]}(P, k)$ has poles¹ whenever the total-momentum squared corresponds to the square of a bound-state mass in this channel (e.g. [66] and references therein). If there exists a bound state and the corresponding on-shell condition, in Euclidean space $P^2 = -M^2$, is met, the properties of the bound state are described by the pole residues of Eq. (1). These residues, the homogeneous BSAs $\Gamma_{[2h]}(k, P)$, can be obtained from the corresponding homogeneous BSE,

$$\Gamma_{[2h]}(k, P) = \int_q K_{[2]}(k, q, P) S^a(q_+) \Gamma_{[2h]}(q, P) S^b(q_-), \quad (2)$$

depicted in Fig. 2.

For Baryons, an analogous construction can be made, where the homogeneous equation for the on-shell amplitude is a covariant three-quark equation often referred to

¹It should be noted that this formalism is also applicable to resonances, where instead of a pole in $\Gamma_{[2]}(P, k)$ as a function of a real variable P^2 one expects a finite peak.

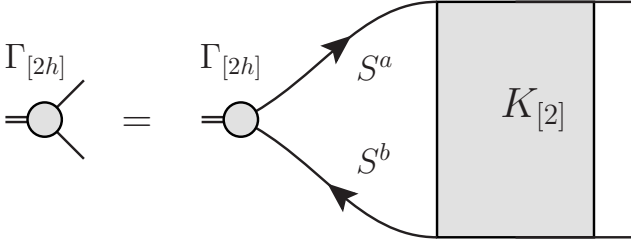


Figure 2: The homogeneous BSE, Eq. (2)

as a covariant Faddeev equation [41, 67, 68], which may be written as

$$\Gamma_{[3h]}(k_1, k_2, P) = \int_{q_1, q_2} S^a(p_1) S^b(p_2) S^c(p_3) \times K_{[3]}(k_1, k_2, q_1, q_2, P) \Gamma_{[3h]}(q_1, q_2, P), \quad (3)$$

and a pictorial representation is given in Fig. 3. Here, the kernel $K_{[3]}(k_1, k_2, q_1, q_2, P)$ subsumes all interactions of the three quarks with the individual momenta p_i , $i = 1, 2, 3$, and the bound state is described by the covariant three-quark on-shell amplitude $\Gamma_{[3h]}(k_1, k_2, P)$, which depends on the total momentum P as well as two relative (Jacobi) momenta k_1 and k_2 . Note that this equation contains an integral over two momenta, namely q_1 and q_2 , thus inflating the size of the problem in terms of a numerical setup.

While in this work we will focus on the solution of bound-state equations such as (1) or (2), a note on the construction of the interaction kernels K and the origin of the quark propagators S as inputs in these equations is in order. In QCD, in addition to the set of DSEs, the Green functions of the theory also satisfy Ward-Takahashi- and/or Slavnov-Taylor identities, e.g. [29, 30]. These relate certain Green functions among each other and provide guidance or even constraints in many cases, if one is to use a truncation and wants to make an Ansatz for, say, $K_{[2]}$. For light-hadron physics, the axial-vector Ward-Takahashi identity is of particular interest, since it encodes the chiral symmetry of QCD with massless quarks as well as its dynamical breaking (see, e.g. [44, 69] for details). In other words, satisfaction of this identity guarantees that the properties of the pion, the lightest hadron and would-be Goldstone boson of dynamical chiral symmetry breaking follow the expected pattern, e.g. the pion mass vanishes in the chiral limit, and leads to a generalized Gell-Mann–Oakes–Renner relation valid for all pseudoscalar mesons [69, 70]. The rainbow-ladder truncation of the DSE-BSE system satisfies the axial-vector Ward-Takahashi identity. Beyond rainbow-ladder truncation, satisfaction of this identity can be achieved on more general terms and has been implemented throughout light-hadron studies of the past years in this approach, e.g. [60–64, 71–73].

More concretely, the satisfaction of this identity leads

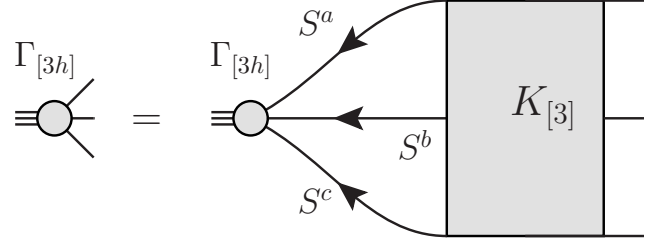


Figure 3: The homogeneous equation for a three-body bound state (covariant Faddeev equation), Eq. (3)

to a close relation of the interaction kernel $K_{[2]}$ in the quark-antiquark BSE and the quark self-energy present in the DSE of the quark propagator, the QCD gap equation. The consistent use of such related kernels in the BSE and the gap equation provides the proper input for the BSE in terms of the quark propagators S as solutions of the symmetry-preserving version of the gap equation. This consistency can be maintained also in numerical studies with high accuracy. In the following we always assume that the gap equation has been solved with the appropriate self-energy to match $K_{[2]}$ and that the resulting quark propagator S is known numerically.

Note that in all bound state equations the real momentum-integration variables and the imaginary total on-shell momentum of the bound state are combined in the (anti-)quark momenta q_{\pm} and q_1, q_2, q_3 to complex four-vectors. As a consequence, the arguments of the dressing functions in the quark propagator become complex. In the meson BSE, for example, the dressing functions are needed in a parabolic region in the complex plane defined by q_{\pm}^2 . Over the past years reliable numerical approaches to this problem have been developed and the required computations are well under control (for more details see [74–76]).

In this way, with the specification of the truncation used, one both decides the structure of the interaction kernel and obtains the quark propagator consistent with this kernel.

3. Numerical representation

The first step towards a numerical representation of Eqs. (1), (2), and (3) is the analysis of the Lorentz and Dirac structure of the respective amplitudes. This structure is a result of the particular representation properties of the state under consideration under the Lorentz group, including the state's parity and spin. Therefore, the bound state amplitudes are decomposed into Lorentz-covariant parts T_i and Lorentz-invariant parts F^i , respectively, reading

$$\Gamma = \sum_{i=1}^N T_i F^i, \quad (4)$$

where the number of terms N as well as the tensor structure of the T_i and Γ depend on the quantum numbers of

the bound state and all arguments have been suppressed for simplicity. The T_i are usually referred to as *covariants*, whereas we call the F^i the *components* of the amplitude Γ . The T_i represent a spin-determined basis for the bound state, and one is — to some extent — free to choose the details thereof.

To be more concrete, we consider the case of mesons in more detail, where two spin-1/2 fermions (the quark and antiquark) are combined to a boson with total spin J . As a result one obtains a 4×4 -matrix structure with the correct Lorentz-transformation properties for a particle of spin J , see e.g. [37]. Consequently one has, in addition to the total meson momentum P^μ and the relative momentum q^μ between the constituents, another four vector γ^μ of Dirac matrices to construct the elements of the BSA. The various combinations of the momenta and γ^μ correctly encode the angular momentum structures inside the meson, i.e. the contributions of (anti-)quark spin and orbital angular momentum.

A scalar meson BSA, for example contains all possible Lorentz-scalar combinations of the three four-vectors P , q , and γ (the actual construction is given below for a pseudoscalar meson in Eqs. (17)-(20)). For the moment we note that while Γ and the T_i in Eq. (4) in general depend on the three four-vectors P , q , and γ as such (which we denote by semicolons between arguments of an expression), the components, being Lorentz- and Dirac-scalars, can only depend on scalar products of the momenta involved, i.e. P^2 , q^2 , and $q \cdot P$ in the meson case. Thus, writing arguments explicitly, Eq. (4) reads

$$\Gamma(\gamma; q; P) = \sum_{i=1}^N T_i(\gamma; q; P) F^i(P^2, q^2, q \cdot P), \quad (5)$$

where again the tensor structure of the T_i (and correspondingly Γ) was not denoted explicitly, since it is irrelevant to the following argument.

In a numerical study, it is mostly advantageous to use a basis that is orthonormal, meaning the covariants satisfy

$$\text{Tr}(T_i \cdot T_j) = \delta_{i,j}, \quad (6)$$

which also defines a generalized scalar product on the space of 4×4 matrices (any occurring Lorentz indices are understood to be summed over here). Note that, for a set of covariants which is neither orthogonal nor normalized, the following step is more involved and we detail it in Appendix C. If one uses the decomposition (4), the bound state equations (1), (2), and (3) can be rewritten as coupled integral equations of the components depending on the scalar products of the momenta via the corresponding projections on the basis T_i .

More concretely, we consider the integrand in, e.g. the (in-)homogeneous meson BSE,

$$K_{[2]}(\gamma; k; q; P) S^a(\gamma; q; P) \Gamma_{[2]}(\gamma; q; P) S^b(\gamma; q; P). \quad (7)$$

The amplitude $\Gamma_{[2]}(\gamma; q; P)$ expanded in the chosen Dirac basis $T_j(\gamma; q; P)$ and the result is projected on $T_i(\gamma; k; P)$.

Doing so, one obtains a matrix structure in the space of covariants, and Eq. (7) can be written as a matrix-vector multiplication in this space involving the BSE *kernel matrix* $K_j^i(k; q; P)$:

$$K_j^i(k; q; P) F^j(P^2, q^2, q \cdot P) = \text{Tr} [T_i(\gamma; k; P) K_{[2]}(\gamma; k; q; P) S^a(\gamma; q; P) \times T_j(\gamma; q; P) S^b(\gamma; q; P)] F^j(P^2, q^2, q \cdot P), \quad (8)$$

where the sum over the repeated index j is implied.

The index j of the components $F^j(P^2, q^2, q \cdot P)$ can thus be viewed as a vector index, which has to be contracted with the corresponding index of the kernel matrix $K_j^i(k; q; P)$. Note that this procedure, although exemplified here for the case of mesons, is completely general, i.e., it applies to baryons as well and is valid for any choice of the interaction kernel K .

The next step is to make the dependence on the continuous momentum variables P^2 , q^2 , and $q \cdot P$ numerically accessible. To achieve this, we apply the so-called Nyström or quadrature method (cf. [77, Chap. 4]), which amounts to replacing an integral by a sum over suitable quadrature weights and points and neglecting the error term. Applying this method discretizes the integration variables, and consequently also the momentum dependence on the left hand side. The homogeneous and the inhomogeneous bound state equations can then be written as matrix equations in the covariants and the discretized momenta and read

$$F_{[h]}^{i,\mathcal{P}} = K_{j,\mathcal{Q}}^{i,\mathcal{P}} F_{[h]}^{j,\mathcal{Q}} \quad (9)$$

in the homogeneous case, and

$$F^{i,\mathcal{P}} = F_0^{i,\mathcal{P}} + K_{j,\mathcal{Q}}^{i,\mathcal{P}} F^{j,\mathcal{Q}} \quad (10)$$

in the inhomogeneous case. The indices i, j label the components, the multi-indices \mathcal{P}, \mathcal{Q} stand for all discretized momentum variables (summation over repeated indices is implied). The matrix $\mathbf{K} = K_{j,\mathcal{Q}}^{i,\mathcal{P}}$ is the same in both equations, and subsumes the interaction kernel, the dressed propagators of the constituents, the Dirac- and Lorentz structure, as well as the discretized integrations. It is applied to a vector $F^{i,\mathcal{P}}$ representing the homogeneous or inhomogeneous bound state amplitude.

As an alternative to the Nyström method, one can expand the momentum dependence of the components into suitable sets of orthogonal functions, which can then be integrated. In this approach, the index \mathcal{P} of the vector $F^{i,\mathcal{P}}$ contains the coefficients of the expansion rather than the values of the components at certain points in momentum space (for applications in the present context, see e.g. [78, 79]).

A partial application of this alternative is the use of a Chebyshev expansion of the dependence in an angle variable as described in Appendix A, where one only keeps a finite number of Chebyshev moments in the representation of the amplitude. This step has been widely used in

DSE studies of hadron spectra and properties, and the fidelity of the approximation investigated in detail, see e.g. [44, 80, 81]. While for studies of hadron masses a few moments are sufficient, more are required in situations where considerable changes of the frame of reference are needed, such as form factor calculations at large momentum transfer [82]; ultimately, in these situations the approximation needs to be abandoned [53, 83].

4. Solution methods

4.1. Homogeneous equations: eigenvalue algorithms

With the results of the preceding section, the homogeneous bound state equation (BSE or Faddeev equation), given in Eq. (9) in index notation, can be written as

$$\vec{F}_{[h]} = \mathbf{K} \cdot \vec{F}_{[h]} \quad (11)$$

using matrix-vector notation. As already mentioned in Sec. 2, this equation is only valid at the on-shell points of the bound states in the respective channel, i.e. at certain values of the total momentum squared $P^2 = -M_n^2$, where $n = 0, 1, 2, \dots$ numbers the ground- and all excited states in the channel. To find such a value of P^2 , one investigates the spectrum of \mathbf{K} as a function of P^2 , since Eq. (11) corresponds to an eigenvalue equation (with the dependence on P^2 made explicit)

$$\lambda(P^2)\vec{F}_{[h]}(P^2) = \mathbf{K}(P^2) \cdot \vec{F}_{[h]}(P^2), \quad (12)$$

where the eigenvalue $\lambda(P^2) = 1$. In other words, to numerically approach a solution of the equation, a part of the result has to be already known, namely the values M_n^2 , or — more precisely — the mass of the state one is looking for. The way out is a self-consistency argument, where the eigenvalue spectrum is plotted as a function of P^2 and those points with $\lambda_n(P^2) = 1$ are identified: the largest eigenvalue determines the ground state, the smaller ones in succession the excitations of the system (see also Fig. 4 below). Typically, one is interested in roughly up to five eigenvalues, since higher excitations are both not well-enough understood in theory and hard to access experimentally.

A great variety of algorithms is available to numerically tackle these kinds of problems, and the most commonly used is a simple iterative method. Similar to the other algorithms discussed in this section, it relies on the multiplication of the matrix \mathbf{K} on a vector and can successively be applied to find also excited states, by projecting on states already obtained, see e.g. [84]. This simple method, however, is not able to resolve pairs of complex conjugate eigenvalues, which may, for example, occur in the meson BSE [85]. In addition, the total number of required matrix-vector multiplications increases for every additional eigenvalue, as demonstrated in Sec. 5.

These difficulties are overcome by the use of more advanced algorithms. For this purpose, we use the implicitly

restarted Arnoldi factorization [86], which is frequently applied in lattice QCD studies, e.g. [87]. An application of this algorithm to bound state calculations is demonstrated in Sec. 5, where we use it to solve the pseudoscalar-meson BSE and compare the efficiency of both methods.

4.2. Inhomogeneous equations: matrix inversion

In the most compact notation, the inhomogeneous bound state equation can be written as

$$\vec{F}(P^2) = \vec{F}_0(P^2) + \mathbf{K}(P^2) \cdot \vec{F}(P^2) \quad (13)$$

where the matrix $\mathbf{K}(P^2)$ is identical to the one in Eq. (11), and the vector \vec{F}_0 is given by the decomposition of Γ_0 according to Eq. (4), $\Gamma^0 = \sum_i T_i F_0^i$ together with the discretization of a possible momentum dependence.

Again, the simplest method to treat this problem is a direct iteration. Mathematically, this corresponds to the representation of the solution by a von Neumann series (cf. [77, Chap. 4]), which can be shown to converge as long as the norm of the operator \mathbf{K} is smaller than one, $\|\mathbf{K}\| < 1$. For matrices, this norm can be related to the largest eigenvalue, such that for $P^2 > -M_0^2$, the iteration converges. When P^2 approaches the ground state position $-M_0^2$ from above, the number of iterations necessarily grows, and no convergence is obtained if $P^2 \leq -M_0^2$, as demonstrated in Sec. 5.

However, a solution is possible for any P^2 if one rewrites Eq. (13) as

$$\vec{F} = (\mathbf{1} - \mathbf{K})^{-1} \cdot \vec{F}_0, \quad (14)$$

i.e., \vec{F} is given by the inhomogeneous term \vec{F}_0 multiplied by the matrix inverse of $(\mathbf{1} - \mathbf{K})$. \vec{F} can then be computed by e.g. inverting the matrix exactly, which has been successfully used to resolve bound-state poles in the inhomogeneous amplitude, as shown in [66] in the case of mesons. On the downside, the direct inversion of a matrix is computationally expensive, and it is not straightforward to parallelize the procedure.

A better approach is to view Eq. (14) as a linear system whose solution is to be found. Equations like this are very common and several algorithms have been developed for their solution. In particular, if the matrix $(\mathbf{1} - \mathbf{K})$ is big, Eq. (14) is a typical application for the so-called Conjugate Gradient (CG) algorithms. Many types of these iterative Krylov-space methods are available. In the case of the bound-state equations considered here, the matrices involved are neither hermitian nor symmetric, such that a good choice is the well-known Bi-Conjugate-Gradients stabilized (BiCGstab) algorithm [88], which is widely used for example in lattice QCD (cf. [19, Chap. 6.2], where also the algorithm is presented in detail).

5. Application: numerical solution of the meson BSE

As an illustration, we apply the algorithms discussed above to solve the homogeneous and inhomogeneous

pseudoscalar-meson BSEs and compare their efficiency in terms of the number of matrix-vector multiplications needed to achieve a specified accuracy. For bigger problems like baryons in a three-quark setup, the kernel matrix typically does not fit into memory, and thus has to be recomputed on the fly in each iteration- or matrix-vector multiplication step. In this case, one matrix-vector multiplication is rather time consuming and it is desirable to keep the number of necessary multiplications as small as possible.

For our test case here, however, we study the pseudoscalar-meson BSE, where the kernel matrix is small, but one can still investigate the questions at hand. We employ the rainbow-ladder truncation, i.e. the rainbow approximation in the quark propagator DSE together with a ladder truncation of the corresponding quark-antiquark BSE. We define the difference in relative momenta $k - q =: \ell$ and the transverse projector with respect to the momentum q as $T^{\mu\nu}(q) := \left(\delta_{\mu\nu} - \frac{q_\mu q_\nu}{q^2} \right)$. In this truncation, the kernel $K_{[2]}(\gamma; k; q; P)$ of the BSEs, Eqs. (1) and (2) is then given by

$$K_{[2]}(\gamma; k; q; P) = -\gamma_\mu \frac{\mathcal{D}(\ell^2)}{\ell^2} T^{\mu\nu}(\ell) \gamma_\nu. \quad (15)$$

where the effective interaction as a function of the momentum-squared s , introduced in Ref. [45], reads

$$\mathcal{D}(s) = D \left(\frac{4\pi^2}{\omega^6} s e^{-s/\omega^2} \right) + \mathcal{F}_{UV}(s). \quad (16)$$

The term $\mathcal{F}_{UV}(s)$ implements the perturbative running coupling of QCD for large s , preserving the one-loop renormalization-group behavior of QCD. The Gaussian term models the enhancement in the intermediate-momentum regime necessary to produce a reasonable amount of dynamical chiral symmetry breaking. It contains the parameters of the model, D and ω , describing the overall strength and momentum-space width (corresponding to an inverse effective range) of the interaction. The behavior of the effective interaction in the far infrared is expected to be of minor relevance to ground-state properties (cf. [89] and references therein). For the present study, we make a common choice for the parameters, namely $D = 0.93 \text{ GeV}^2$ and $\omega = 0.4 \text{ GeV}$ (for full details on the truncation, the effective coupling, or the effects of other parameter values, see e.g. [39, 44, 45]).

5.1. Kernel setup

The above definitions together with the dressed quark propagators computed already completely specify the ingredients of the BSE. We investigate light quarks in analogy to [39], where the current-quark mass in an isospin-symmetric setup was adjusted to fit the bound-state mass of the ρ meson. The details of the discretization of the

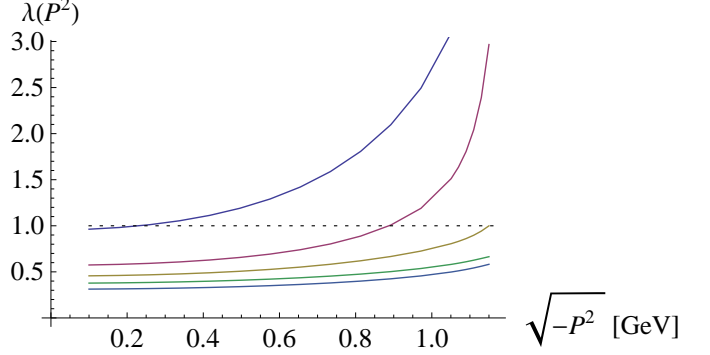


Figure 4: The five largest eigenvalues of the homogeneous BSE plotted over $\sqrt{-P^2}$ which corresponds to the bound state mass M where $\lambda = 1$ indicated by the horizontal dashed line. The ground-state (leftmost intersection) solution vector has positive C -parity (pion), the second has negative (exotic) and the third again has positive C -parity (excited pion).

kernel matrix proceed as follows: The orthonormal pseudoscalar covariants, constructed to satisfy Eq. (6), read

$$T_1 = \frac{\gamma_5}{2}, \quad (17)$$

$$T_2 = \frac{\gamma_5(\gamma \cdot P)}{2\sqrt{-P^2}}, \quad (18)$$

$$T_3 = \frac{\gamma_5((\gamma \cdot q) - \frac{(\gamma \cdot P)(P \cdot q)}{P^2})}{2\sqrt{\frac{(P \cdot q)^2}{P^2} - q^2}}, \quad (19)$$

$$T_4 = \frac{\frac{1}{2}i\gamma_5((\gamma \cdot q)(\gamma \cdot P) - (\gamma \cdot P)(\gamma \cdot q))}{2\sqrt{P^2 q^2 - (P \cdot q)^2}}. \quad (20)$$

Choosing the rest frame of the quark-anti-quark system, and applying the parametrization and discretization as described in Appendix A, the kernel matrix Eq. (8) in our setup becomes

$$\begin{aligned} \mathbf{K} &= K_{j,l,m}^{i,r,s}(P) = \\ &= \frac{4}{3(2\pi)^3} w[q_l^2] w[z_m] \int_{-1}^1 dy \frac{\mathcal{D}(\ell^2)}{\ell^2} T^{\mu\nu}(\ell) \\ &\times \text{Tr}[T_i(\gamma; k; P) \gamma_\mu S(q_+) T_j(\gamma; q; P) S(q_-) \gamma_\nu], \end{aligned} \quad (21)$$

where $w[q_l^2]$, $w[z_m]$ denote the quadrature weights and the replacements $k^2 \rightarrow k_r^2$, $z_k \rightarrow z_s$, $q^2 \rightarrow k_l^2$, $z \rightarrow z_m$ have been made in all occurring momenta to implement the discretization. Therefore, the indices i, j label the components and r, s, l, m the momentum space points. For the following calculations, we use $N_q = 32$ and $N_z = 24$, such that \mathbf{K} has the dimensions $(32, 24, 4) \times (32, 24, 4)$.

5.2. Homogeneous BSE

To solve the homogeneous BSE, we use both the MPI based version of the ARPACK library (an implementation of the implicitly restarted Arnoldi factorization) and the simple iteration. Fig. 4 shows the largest five eigenvalues

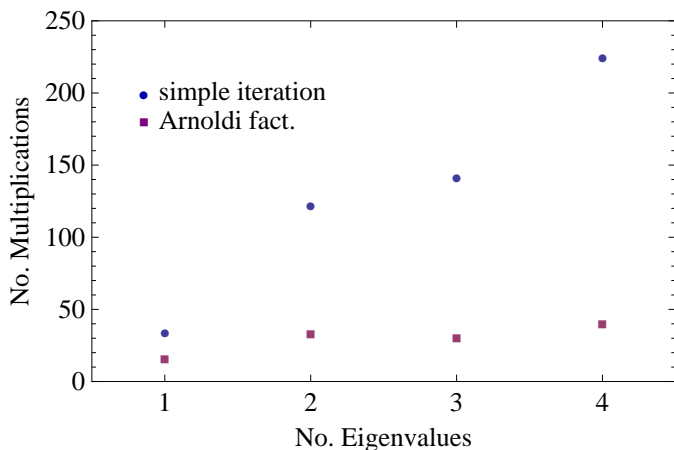


Figure 5: The number of matrix-vector multiplications needed for convergence of the simple iteration (circles) and the Arnoldi factorization (squares), plotted against the number of eigenvalues computed at a (typical) fixed value of $P^2 = -M_0^2$.

of \mathbf{K} for our example. Bound-state masses can be identified by the positions at which an eigenvalue curve crosses one (dashed line in the figure) and from left to right correspond to the ground- and first-excited, second-excited, etc., states. Note that in our approach we do not restrict the symmetry of the amplitudes (eigenvectors) with respect to the angular variable z , such that we obtain homogeneous solutions of both positive and negative charge-conjugation parity (C -parity) for equal-mass constituents and a choice of $1/2$ for the momentum-partitioning parameters η_{\pm} , as indicated above (for more details on the definition and calculation of C , see Appendix B). In the pseudoscalar case, a negative C -parity is considered *exotic*, since it is not available for a $\bar{q}q$ state in quantum mechanics. However, it appears naturally in a quark-antiquark BSE setup, where our main interest here comes from a systematic point of view. A more general discussion of states with exotic C -parity in this formalism and their possible interpretations can be found, e.g., in [37, 85, 90, 91].

To compare the efficiency of the two algorithms, Arnoldi factorization versus iteration, we compute the one to four largest eigenvalues of \mathbf{K} and compare the convergence in terms of the number of iterations needed to obtain an absolute accuracy of the eigenvector of $\epsilon = 10^{-8}$, at a typical value of $P^2 = -M_0^2 = 0.0527 \text{ GeV}^2$. The results, given in Fig. 5, show that for the first eigenvalue the Arnoldi factorization needs only half as many matrix-vector multiplications as the simple iteration. With increasing number of eigenvalues, the use of this advanced algorithm becomes even more advantageous.

Another interesting observation from Fig. 5 is that the Arnoldi factorization was more efficient for three eigenvalues than when only two were requested. This is most likely due to a “clustering” of eigenvalues number two and three for the algorithm, an effect which appears for eigenvalues

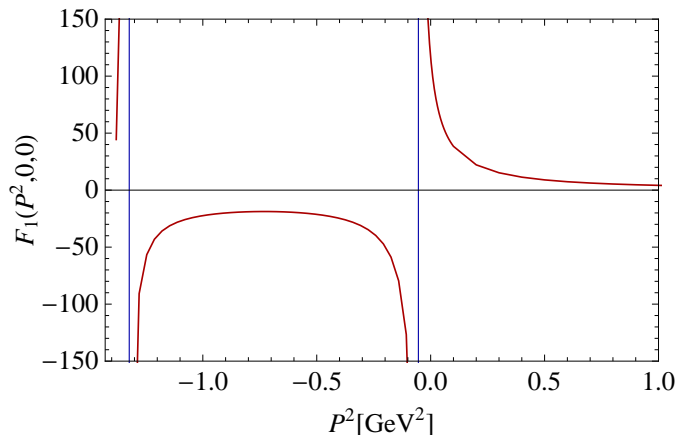


Figure 6: Component $F_1(P^2, 0, 0)$ of the inhomogeneous pseudoscalar amplitude calculated using BiCGstab vs. the square of the total momentum P^2 . The vertical lines mark the pole positions, corresponding to the pion ground- and first excited state ($J^{PC} = 0^{+-}$).

close together and is also related to the eigenvectors. In this particular case, eigenvectors two and three have opposite C -parity or z -symmetry, which may make them more easily distinguishable for the algorithm and more easy to obtain as a result. The ARPACK library is very efficient at evaluating all eigenvalues in such a cluster, while convergence is slower, if one asks for only one or a few of the eigenvalues in the cluster (see also the ARPACK users guide [92]).

5.3. Inhomogeneous BSE

We apply the direct iteration (summation of the von Neumann series) and the inversion using the BiCGstab algorithm to solve the inhomogeneous BSE (1), in the setup described above for pseudoscalar quantum numbers.

In the inhomogeneous case not only the structure of the amplitude determines the quantum numbers of the solution but also that of the inhomogeneous term Γ_0 . Following [69], a possible choice for pseudoscalars is

$$\Gamma_0 = Z_4 \gamma_5, \quad (22)$$

where Z_4 is a renormalization constant obtained from the gap equation (cf. [44]). With this choice (pseudoscalar, positive C -parity), no poles corresponding to negative C -parity appear in the solution, as can be seen from Fig. 6. The curve shown in this figure has been obtained with the BiCGstab algorithm, because as described in Sec. 4.2 the direct iteration fails to converge if $P^2 \leq -M_0^2$. This is demonstrated in Fig. 7, where the number of matrix-vector multiplications needed for convergence is plotted against P^2 for both methods.

It is clear that the number of matrix-vector multiplications needed for the direct iteration diverges as P^2 approaches $-M_0^2$ (note that Fig. 7 uses a logarithmic scale on the vertical axis). The inversion with BiCGstab, however, converges for all P^2 with nearly the same speed, needing approximately 10 matrix-vector multiplications.

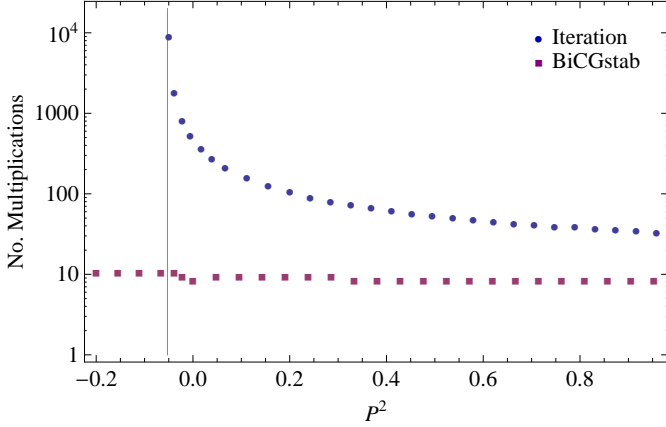


Figure 7: The number of matrix-vector multiplications needed for convergence of the iterative solution of Eq. (1) (circles) and the BiCGstab algorithm (squares), plotted on a logarithmic scale against the square of the total momentum P^2 of the amplitude. The vertical line indicates the position of the ground state $P^2 = -M_0^2$ of the system. Note that the straightforward iteration does not converge for $P^2 \leq -M_0^2$.

6. Conclusion and Outlook

We have investigated aspects and benefits of different numerical solution methods for the pseudoscalar meson BSE in a rainbow-ladder truncation of the DSE approach to QCD. In a realistic model, our comparison was aimed at a small-scale test and subsequent identification of efficient algorithms for the numerical approach to bound-state problems in this covariant continuum approach to a quantum field theory. Since the algorithms used and advocated are applicable in a very general way to the matrix representations of the integral kernels appearing in such bound-state studies, the strategies proposed here are valuable for similar studies of bound states in more involved truncations than rainbow-ladder on one hand.

On the other hand, any bound-state problem involving more than two constituents, starting with but not limited to baryons in a three-quark setup, needs efficient methods to perform sophisticated numerical studies, given the computational resources presently available. In general one will find that in both examples given here one simply has to deal with a larger kernel matrix and thus efficiency of the algorithms used is of the essence.

One particularly interesting observation with regard to present-day covariant three-quark studies is that computing bound-state masses is more efficient using the inhomogeneous equation than the homogeneous one. In addition, the kernel matrices often need to be constructed on the fly due to limited system memory. With these two aspects combined, such a problem appears to be an ideal application for the field of GPU computing.

Appendix A. Aspects of four-dimensional momentum integration

We use 4-dim. spherical coordinates, such that the momentum integration is written as

$$\int_{-\infty}^{\infty} d^4 q \rightarrow \int_0^{\infty} d(q^2) \frac{q^2}{2} \int_{-1}^1 dz \sqrt{1-z^2} \int_{-1}^1 dy \int_0^{2\pi} d\phi. \quad (\text{A.1})$$

In the meson BSE, there are three relevant momenta: P (total momentum), k (relative momentum), and q (loop momentum). Subsequently, we choose P to be in the rest-frame of the bound state,

$$P = (0, 0, 0, \sqrt{P^2}). \quad (\text{A.2})$$

The other momenta are chosen accordingly and read

$$k = \sqrt{k^2} \left(0, 0, \sqrt{1-z_k^2}, z_k \right) \quad (\text{A.3})$$

and

$$q = \sqrt{q^2} \left(0, \sqrt{1-z^2} \sqrt{1-y^2}, \sqrt{1-z^2} y, z \right). \quad (\text{A.4})$$

In this parametrization, the integration $\int d\phi$ is trivial.

The components of the amplitude on the left hand side of the BSEs Eqs. (1) and (2) depend on the scalar products $P \cdot k = z_k \sqrt{k^2} \sqrt{P^2}$, P^2 , and k^2 . Inside the integral, on the right hand side, the scalar products become $P \cdot q = z \sqrt{q^2} \sqrt{P^2}$, P^2 , and q^2 . Thus, the BSE kernel matrix \mathbf{K} induces the following mapping on the momentum variables

$$(q^2, z) \mapsto (k^2, z_k), \quad (\text{A.5})$$

such that the integration $\int dy$ does not add a dimension \mathbf{K} , although it is not trivial.

After choosing a parametrization of the momentum integration, the next step is to discretize the momentum dependence. In this work, we straightforwardly apply the quadrature method, and replace

$$\int_0^{\infty} d(q^2) \frac{q^2}{2} \int_{-1}^1 dz \sqrt{1-z^2} \rightarrow \sum_{l=1}^{N_q} \sum_{m=1}^{N_z} w[q_l^2] w[z_m], \quad (\text{A.6})$$

where $w[q_l^2]$, $w[z_m^2]$ denote the quadrature weights and q_l^2 , z_m the corresponding nodes. The factors of $q^2/2$ and $\sqrt{1-z^2}$ have been absorbed in the weights.

Note that, especially for the integration over z , it is advantageous to use a quadrature rule whose weights include $\sqrt{1-z^2}$ by construction, e.g., the Gauss-Chebyshev type 2 rule.

An alternative, advantageous and widely used in the calculations of hadron spectra is to apply the quadrature method discussed above only to $\int d(q^2)$ and to resolve the z -dependence and by an expansion in Chebyshev polynomials of the second kind. The components are then written as

$$F^i(P^2, q^2, z) = \sum_{m=1}^M {}^m F_i(q^2, P^2) U_m(z), \quad (\text{A.7})$$

with ${}^m F_i(q^2, P^2)$ the so-called Chebyshev *moments*, which retain only the functional dependence on k^2 and P^2 . The number of terms M taken into account is finite in practice, but infinite in principle. The Chebyshev polynomials of the second kind $U_m(z)$ satisfy the orthogonality relation

$$\frac{2}{\pi} \int dz \sqrt{1-z^2} U_m(z) U_n(z) = \delta_{mn} . \quad (\text{A.8})$$

To obtain a matrix structure not only in the covariants, but also in the Chebyshev moments, the above expansion is inserted in Eq. (8), and is then projected on one moment by use of Eq. (A.8). This finally leads to

$$\begin{aligned} \int_q K_{j,n}^{i,m}(k; q; P) {}^n F_j(q^2, P^2) = \\ \left(\frac{2}{\pi} \int_q \int_{-1}^1 dz_k U_m(z_k) \text{Tr} [T_i(\gamma; k; P) K_{[2]}(\gamma; k; q; P) \times \right. \\ \left. S^a(\gamma; q; P) T_j(\gamma; q; P) S^b(\gamma; q; P)] U_n(z) \right) {}^n F_j(q^2, P^2) . \end{aligned} \quad (\text{A.9})$$

Again, the sum over the repeated indices j, n is implied.

Appendix B. (Generalized) C -parity

The action of the C -parity transformation on the meson BSA is defined via

$$\bar{\Gamma}(P; k) = (C \Gamma(P; -k) C^{-1})^t , \quad (\text{B.1})$$

where t denotes the matrix-transpose, and the charge-conjugation matrix $C = \gamma_2 \gamma_4$. If the C -parity is a good quantum number of the system, $\Gamma(P; k)$ is an eigenstate of the C -parity operation given above, with eigenvalues $\lambda_C = \pm 1$,

$$(C \Gamma(P; -k) C^{-1})^t = \lambda_C \Gamma(P; k) . \quad (\text{B.2})$$

The amplitudes occurring in Eq. (B.2) can be decomposed into covariants and components according to Eq. (5), such that in the rest frame of the bound state with the notation introduced in Eqs. (A.2) - (A.4),

$$\begin{aligned} \sum_{i=1}^N (C T_i(P; -k) C^{-1})^t F^i(P^2, k^2, -z_k) \\ = \lambda_C \sum_{i=1}^N T_i(P; k) F^i(P^2, k^2, z_k) . \end{aligned} \quad (\text{B.3})$$

Projecting this equation on one covariant using the orthogonality relation (6), we obtain

$$\begin{aligned} \bar{F}^j(P^2, k^2, z_k) := \\ \sum_{i=1}^N \text{Tr} [T_j(P; k) (C T_i(P; -k) C^{-1})^t] F^i(P^2, k^2, -z_k) \\ = \lambda_C F^j(P^2, k^2, z_k) . \end{aligned} \quad (\text{B.4})$$

The next step is to discretize the momenta using the quadrature method, such that the functional dependence of the component vectors on the momentum variables can be represented in index notation,

$$F^j(P^2, k^2, z_k) \Rightarrow F^{j,l,m} , \quad (\text{B.5})$$

$$\bar{F}^i(P^2, k^2, z_k) \Rightarrow \bar{F}^{i,l,m} . \quad (\text{B.6})$$

Now, the amplitudes are given as complex vectors, such that the canonical scalar product on \mathbf{C}^n can be used to solve for λ_C ,

$$\lambda_C = \frac{\bar{F}^{j,l,m} (F^{j,l,m})^*}{\bar{F}^{i,r,s} (F^{i,r,s})^*} , \quad (\text{B.7})$$

where $*$ denotes complex conjugation, and repeated indices are summed over.

For states with definite C -parity $\lambda_C = \pm 1$. As can be seen from the above equations, the C -parity is determined by the (anti)-symmetry of the amplitudes with respect to z_k . For states which are not eigenstates of the C operation, Eq. (B.7) can be used to *define* a "generalized C -parity". It lies between -1 and 1 , and its deviation from these values indicates the asymmetry of the state caused, e.g., by mass difference of the constituents.

It is interesting to note that the C -parity as a symmetry property of the eigenvectors of \mathbf{K} is constant over the whole range of P^2 , even if the on-shell condition for this state is not fulfilled, i.e. $P^2 \neq -M^2$.

Appendix C. Using a non-orthogonal Dirac basis

Consider the inhomogeneous BSE written in the general form

$$\begin{aligned} f(\gamma; k; P) \Gamma(\gamma; k; P) = Z(\gamma; k; P) \\ - \int_q K_1(\gamma; k; q; P) \Gamma(\gamma; q; P) K_2(\gamma; k; q; P) , \end{aligned} \quad (\text{C.1})$$

where the dependence of every term on all variables including γ matrices is given explicitly. The $;$ between variables again denotes a dependence on complete four-vectors. K_1 and K_2 represent generalized formal kernel pieces, Z a general driving term, and f an arbitrary function of its arguments. To transform this equation into a set of coupled integral equations for components and then use Chebyshev moments, which are described in Appendix A, we write the BSA as the sum over its covariants T_i and Lorentz- as well as Dirac-scalar components F^i and the latter as sums over Chebyshev polynomials and moments

$$\Gamma(\gamma; k; P) = \sum_{i=1}^M \sum_{j=1}^N T_j(\gamma; k; P) {}^i F_j(k^2, P^2) U_i(z_k) , \quad (\text{C.2})$$

where M is the number of Chebyshev polynomials taken into account and N is the number of covariants in the BSA. The Chebyshev polynomial of the second kind $U_i(z_k)$ depends on $z_k := k \cdot P / \sqrt{k^2 P^2}$. Now we apply $T_n(\gamma; k; P)$

on Eq. (C.1) from the left and take the Dirac trace. The result is

$$\sum_{i=1}^M \sum_{j=1}^N A_{nj}(k^2, P^2, z_k)^i F_j(k^2, P^2) U_i(z_k) = Z_n(k^2, P^2, z_k) - \sum_{l=1}^M \sum_{m=1}^N \int_q \text{Tr} [T_n(\gamma; k; P) \times K_1(\gamma; k; q; P) T_m(\gamma; q; P) {}^l F_m(q^2, P^2) \times U_l(z_q) K_2(\gamma; k; q; P)] , \quad (\text{C.3})$$

where

$$A_{nj}(k^2, P^2, z_k) := \text{Tr} [T_n(\gamma; k; P) f(\gamma; k; P) T_j(\gamma; k; P)] \\ Z_n(k^2, P^2, z_k) := \text{Tr} [T_n(\gamma; k; P) Z(\gamma; k; P)] \quad (\text{C.4})$$

The next step is to invert the matrix A_{nj} for each set of coordinates (k^2, P^2, z_k) , and apply its inverse to the equation, i.e., $\sum_{n=1}^N A_{rn}^{-1}$ from the left:

$$\sum_{i=1}^M {}^i F_r(k^2, P^2) U_i(z_k) = \sum_{n=1}^N A_{rn}^{-1}(k^2, P^2, z_k) Z_n(k^2, P^2, z_k) \\ - \sum_{n=1}^N \sum_{l=1}^M \sum_{m=1}^N \int_q A_{rn}^{-1}(k^2, P^2, z_k) \text{Tr} [T_n(\gamma; k; P) K_1(\gamma; k; q; P) \times T_m(\gamma; q; P) {}^l F_m(q^2, P^2) U_l(z_q) K_2(\gamma; k; q; P)] \quad (\text{C.5})$$

The last step is the projection with the help of Chebyshev polynomials via $\frac{2}{\pi} \int dz_k \sqrt{1 - z_k^2} U_j(z_k)$ from the left (cf. Eq. (A.8)) and one obtains

$${}^j F_r(k^2, P^2) = V_Z(j, r, k^2) - \sum_{l=1}^M \sum_{n,m=1}^N \frac{2}{\pi} \int_q \int_{z_k} \sqrt{1 - z_k^2} \\ \times U_j(z_k) A_{rn}^{-1}(k^2, P^2, z_k) \text{Tr} [T_n(\gamma; k; P) K_1(\gamma; k; q; P) \times T_m(\gamma; q; P) {}^l F_m(q^2, P^2) U_l(z_q) K_2(\gamma; k; q; P)] \quad (\text{C.6})$$

with the driving term given by

$$V_Z(j, r, k^2) := \frac{2}{\pi} \sum_{n=1}^N \int dz_k \sqrt{1 - z_k^2} U_j(z_k) \\ \times A_{rn}^{-1}(k^2, P^2, z_k) Z_n(k^2, P^2, z_k) . \quad (\text{C.7})$$

This procedure does not require the set of covariants to be orthogonal, it is completely general, also with respect to the kernel, the driving term, and possible terms multiplying the amplitude on the left-hand side of the BSE. All terms and projections are included correctly via the matrix A . In the case considered in the present work, $f = 1$ and the driving term has the standard form for pseudoscalar mesons, Eq. (22).

Acknowledgments

We would like to acknowledge valuable discussions with R. Alkofer, C.S. Fischer, C. Gatttringer, C.B. Lang,

A. Maas, D. Mohler, C.D. Roberts, M. Schwinzerl, and S.V. Wright. This work was supported by the Austrian Science Fund *FWF* under project no. P20496-N16, and was performed in association with and supported in part by the *FWF* doctoral program no. W1203-N08.

References

- [1] W. J. Marciano, H. Pagels, Phys. Rept. 36 (1978) 137.
- [2] D. J. Gross, F. Wilczek, Phys. Rev. Lett. 30 (1973) 1343–1346.
- [3] D. J. Gross, F. Wilczek, Phys. Rev. D 8 (10) (1973) 3633–3652.
- [4] H. D. Politzer, Phys. Rev. Lett. 30 (1973) 1346–1349.
- [5] G. P. Lepage, S. J. Brodsky, Phys. Rev. D 22 (1980) 2157.
- [6] S. Godfrey, N. Isgur, Phys. Rev. D 32 (1985) 189–231.
- [7] S. Capstick, N. Isgur, Phys. Rev. D 34 (1986) 2809.
- [8] L. Y. Glozman, W. Plessas, K. Varga, R. F. Wagenbrunn, Phys. Rev. D 58 (1998) 094030.
- [9] T. Barnes, S. Godfrey, E. S. Swanson, Phys. Rev. D 72 (2005) 054026.
- [10] T. Melde, W. Plessas, B. Sengl, Phys. Rev. D 77 (2008) 114002.
- [11] J. Gasser, H. Leutwyler, Ann. Phys. 158 (1984) 142.
- [12] S. Scherer, Adv. Nucl. Phys. 27 (2003) 277.
- [13] N. Brambilla, et al., arXiv:hep-ph/0412158.
- [14] C. McNeile, C. Michael, Phys. Rev. D 74 (2006) 014508.
- [15] T. Burch, et al., Phys. Rev. D 73 (2006) 094505.
- [16] H. Wada, et al., Phys. Lett. B 652 (2007) 250–254.
- [17] J. J. Dudek, R. G. Edwards, N. Mathur, D. G. Richards, Phys. Rev. D 77 (2008) 034501.
- [18] E. B. Gregory, A. C. Irving, C. McNeile, C. Richards, PoS Lattice2008 (2009) 286.
- [19] C. Gatttringer, C. B. Lang, Lect. Notes Phys. 788 (2010) 1–211.
- [20] P. Colangelo, A. Khodjamirian, arXiv:hep-ph/0010175.
- [21] M. Jamin, B. O. Lange, Phys. Rev. D 65 (2002) 056005.
- [22] K. Maltman, J. Kambor, Phys. Rev. D 65 (2002) 074013.
- [23] A. A. Penin, M. Steinhauser, Phys. Rev. D 65 (2002) 054006.
- [24] P. Ball, R. Zwicky, Phys. Rev. D 71 (2005) 014015.
- [25] W. Lucha, D. Melikhov, H. Sazdjian, S. Simula, Phys. Rev. D 80 (2009) 114028.
- [26] J. M. Pawłowski, Annals Phys. 322 (2007) 2831–2915.
- [27] H. Gies, C. Wetterich, Phys. Rev. D 65 (2002) 065001.
- [28] R. Alkofer, J. Greensite, J. Phys. G 34 (2007) S3.
- [29] C. D. Roberts, A. G. Williams, Prog. Part. Nucl. Phys. 33 (1994) 477–575.
- [30] R. Alkofer, L. von Smekal, Phys. Rept. 353 (2001) 281.
- [31] C. S. Fischer, J. Phys. G 32 (2006) R253–R291.
- [32] P. Maris, C. D. Roberts, Int. J. Mod. Phys. E12 (2003) 297–365.
- [33] C. D. Roberts, M. S. Bhagwat, A. Holl, S. V. Wright, Eur. Phys. J. Special Topics 140 (2007) 53–116.
- [34] C. D. Roberts, S. M. Schmidt, Prog. Part. Nucl. Phys. 45 (2000) S1–S103.
- [35] H. A. Bethe, E. E. Salpeter, Phys. Rev. 82 (1951) 309.
- [36] E. E. Salpeter, H. A. Bethe, Phys. Rev. 84 (1951) 1232–1242.
- [37] C. H. Llewellyn-Smith, Ann. Phys. 53 (1969) 521–558.
- [38] P. Jain, H. J. Munczek, Phys. Rev. D 48 (1993) 5403–5411.
- [39] A. Krassnigg, Phys. Rev. D 80 (2009) 114010.
- [40] L. D. Faddeev, Sov. Phys. JETP 12 (1961) 1014–1019.
- [41] G. Eichmann, R. Alkofer, A. Krassnigg, D. Nicmorus, Phys. Rev. Lett. 104 (2010) 201601.
- [42] R. Alkofer, C. S. Fischer, F. J. Llanes-Estrada, K. Schwenzer, Annals Phys. 324 (2009) 106.
- [43] C. S. Fischer, A. Maas, J. M. Pawłowski, Annals Phys. 324 (2008) 2408–2437.
- [44] P. Maris, C. D. Roberts, Phys. Rev. C 56 (1997) 3369–3383.
- [45] P. Maris, P. C. Tandy, Phys. Rev. C 60 (1999) 055214.
- [46] M. A. Ivanov, Y. L. Kalinovsky, C. D. Roberts, Phys. Rev. D 60 (1999) 034018.
- [47] D. Jarecke, P. Maris, P. C. Tandy, Phys. Rev. C 67 (2003) 035202.
- [48] D. W. Jarecke, Properties of mesons from Bethe-Salpeter amplitudes, Ph.D. thesis, Kent State University (2005).

- [49] M. A. Ivanov, Y. L. Kalinovsky, P. Maris, C. D. Roberts, *Phys. Rev. C* 57 (1998) 1991–2003.
- [50] P. Maris, P. C. Tandy, *Phys. Rev. C* 61 (2000) 045202.
- [51] P. Maris, P. C. Tandy, *Phys. Rev. C* 62 (2000) 055204.
- [52] A. Holl, A. Krassnigg, P. Maris, C. D. Roberts, S. V. Wright, *Phys. Rev. C* 71 (2005) 065204.
- [53] M. S. Bhagwat, P. Maris, *Phys. Rev. C* 77 (2008) 025203.
- [54] M. Oettel, R. Alkofer, *Eur. Phys. J. A* 16 (2003) 95–109.
- [55] R. Alkofer, A. Holl, M. Kloker, A. Krassnigg, C. D. Roberts, *Few-Body Syst.* 37 (2005) 1–31.
- [56] G. Eichmann, A. Krassnigg, M. Schwinzerl, R. Alkofer, *Annals Phys.* 323 (2008) 2505–2553.
- [57] R. Alkofer, G. Eichmann, A. Krassnigg, D. Nicmorus, *Chinese Physics C* 34 (2010) 1175–1180.
- [58] D. Nicmorus, G. Eichmann, R. Alkofer, [arXiv:1008.3184](https://arxiv.org/abs/1008.3184).
- [59] D. Nicmorus, G. Eichmann, A. Krassnigg, R. Alkofer, [arXiv:1008.4149](https://arxiv.org/abs/1008.4149).
- [60] P. Watson, W. Cassing, *Few-Body Syst.* 35 (2004) 99–115.
- [61] P. Watson, W. Cassing, P. C. Tandy, *Few-Body Syst.* 35 (2004) 129–153.
- [62] C. S. Fischer, R. Williams, *Phys. Rev. D* 78 (2008) 074006.
- [63] C. S. Fischer, R. Williams, *Phys. Rev. Lett.* 103 (2009) 122001.
- [64] L. Chang, C. D. Roberts, *Phys. Rev. Lett.* 103 (2009) 081601.
- [65] L. Chang, C. D. Roberts, *AIP Conf. Proc.* 1261 (2010) 25–30.
- [66] M. S. Bhagwat, A. Hoell, A. Krassnigg, C. D. Roberts, S. V. Wright, *Few-Body Syst.* 40 (2007) 209–235.
- [67] G. Eichmann, R. Alkofer, A. Krassnigg, D. Nicmorus, *EPJ Web of Conferences* 3 (2010) 03028.
- [68] G. Eichmann, Hadron properties from QCD bound-state equations, Ph.D. thesis, University of Graz (2009).
- [69] P. Maris, C. D. Roberts, P. C. Tandy, *Phys. Lett. B* 420 (1998) 267–273.
- [70] A. Holl, A. Krassnigg, C. D. Roberts, *Phys. Rev. C* 70 (2004) 042203(R).
- [71] H. J. Munczek, *Phys. Rev. D* 52 (1995) 4736–4740.
- [72] A. Bender, C. D. Roberts, L. Von Smekal, *Phys. Lett. B* 380 (1996) 7–12.
- [73] M. S. Bhagwat, A. Holl, A. Krassnigg, C. D. Roberts, P. C. Tandy, *Phys. Rev. C* 70 (2004) 035205.
- [74] C. S. Fischer, P. Watson, W. Cassing, *Phys. Rev. D* 72 (2005) 094025.
- [75] C. S. Fischer, D. Nickel, R. Williams, *Eur. Phys. J. C* 60 (2008) 1434–6052.
- [76] A. Krassnigg, *PoS Confinement8* (2009) 75.
- [77] L. M. Delves, J. L. Mohamed, *Computational methods for integral equations*, Cambridge University Press, 1985.
- [78] M. Bhagwat, M. A. Pichowsky, P. C. Tandy, *Phys. Rev. D* 67 (2003) 054019.
- [79] S. M. Dorkin, T. Hilger, L. P. Kaptari, B. Kaempfer, [arXiv:1008.2135](https://arxiv.org/abs/1008.2135).
- [80] M. Oettel, L. Von Smekal, R. Alkofer, *Comput. Phys. Commun.* 144 (2002) 63.
- [81] R. Alkofer, P. Watson, H. Weigel, *Phys. Rev. D* 65 (2002) 094026.
- [82] A. Höll, R. Alkofer, M. Kloker, A. Krassnigg, C. D. Roberts, S. V. Wright, *Nucl. Phys. A* 755 (2005) 298–302.
- [83] P. Maris, P. C. Tandy, *Nucl. Phys. Proc. Suppl.* 161 (2006) 136–152.
- [84] A. Krassnigg, C. D. Roberts, *Fizika B* 13 (2004) 143–152.
- [85] S. Ahlig, R. Alkofer, *Annals Phys.* 275 (1999) 113–147.
- [86] D. C. Sorensen, Implicitly restarted Arnoldi/Lanczos methods for large scale eigenvalue calculations, Tech. Rep. TR-96-40, Rice University, Houston, Texas (1996).
[URL citeseer.ist.psu.edu/174335.html](http://citeseer.ist.psu.edu/174335.html)
- [87] M. Joergler, C. B. Lang, *PoS LAT2007* (2007) 107.
- [88] H. A. van der Vorst, *SIAM J. Sci. Stat. Comput.* 13 (2) (1992) 631–644.
- [89] M. Blank, A. Krassnigg, A. Maas, [arXiv:1007.3901](https://arxiv.org/abs/1007.3901).
- [90] N. Nakanishi, *Prog. Theor. Phys. Suppl.* 43 (1969) 1–81.
- [91] C. J. Burden, M. A. Pichowsky, *Few-Body Syst.* 32 (2002) 119–126.
- [92] R. B. Lehoucq, D. C. Sorensen, C. Yang, *ARPACK Users' Guide: Solution of Large-Scale Eigenvalue Problems with Implicitly Restarted Arnoldi Methods*, Society for Industrial & Applied Mathematics, 1998.